Organic Nitrate Aerosol Formation via NO_3 + Biogenic Volatile Organic Compounds in the Southeastern United States

Benjamin R. Ayres[1], Hannah M. Allen[1,2], Danielle C. Draper[1,3], Steven S. Brown[4], Robert J. Wild[4], Jose L. Jimenez[5,6], Douglas A. Day[5,6], Pedro Campuzano-Jost[5,6], Weiwei Hu[5,6], Joost de Gouw[5,6], Abigail Koss[5,6], Ronald C. Cohen[7], Kaitlin C. Duffey[7], Paul Romer[7], Karsten Baumann[8], Eric Edgerton[8], Satoshi Takahama[9], Joel A. Thornton[10], Ben H. Lee[10], Felipe D. Lopez-Hilfiker[10], Claudia Mohr[10,11], Paul O. Wennberg[12], Tran B. Nguyen[12], Alex Teng[12], Allen H. Goldstein[13], Kevin Olson[13], and Juliane L. Fry[1]

[1]Department of Chemistry, Reed College, Portland, OR, USA
[2]Division of Chemistry and Chemical Engineering, California Institute of Technology, Pasadena, CA, USA
[3]Department of Chemistry, University of California, Irvine, CA, USA
[4]Earth System Research Laboratory, National Oceanic and Atmospheric Administration, Boulder, CO, USA
[5]Cooperative Institute for Research in Environmental Sciences, University of Colorado, Boulder, Colorado, USA
[6]Department of Chemistry and Biochemistry, University of Colorado, Boulder, CO, USA
[7]Department of Chemistry, University of California at Berkeley, CA, USA
[8]Applied Research Associates, Inc., Research Triangle Park, N.C., USA
[9]Department of Environmental Engineering, École polytechnique fédérale de Lausanne (EPFL), Switzerland
[10]Department of Atmospheric Sciences, University of Washington, Seattle, WA, USA
[11]Karlsruhe Institute of Technology, Karlsruhe, Germany
[12]Division of Geological and Planetary Sciences and Division of Engineering and Applied Science, California Institute of Technology, Pasadena, CA, USA
[13]Department of Environmental Science, Policy, and Management, University of California, Berkeley, CA, USA

Correspondence to: J. L. Fry (fry@reed.edu)

Abstract.

Gas- and aerosol-phase measurements of oxidants, biogenic volatile organic compounds (BVOC) and organic nitrates made during the Southern Oxidant and Aerosol Study (SOAS campaign, Summer 2013) in central Alabama show that nitrate radical (NO_3) reaction with monoterpenes leads to significant secondary aerosol formation. Cumulative losses of NO_3 to terpenes are correlated with increase in gas- and aerosol-organic nitrate concentrations made during the campaign. Correlation of NO_3 radical consumption to organic nitrate aerosol formation as measured by Aerosol Mass Spectrometry and Thermal Dissociation - Laser Induced Fluorescence suggests a molar yield of aerosol phase monoterpene nitrates of 23-44%. Compounds observed via chemical ionization mass spectrometry (CIMS) are correlated against predicted NO_3 loss to BVOC, and show $C_{10}H_{15}NO_5$ and $C_{10}H_{17}NO_5$ as major NO_3-oxidized terpene products being incorporated into aerosols. The comparable isoprene product $C_5H_9NO_5$ was observed to contribute less than 1% of the total organic nitrate in the aerosol phase and correlations show that it is principally a gas phase product from nitrate oxidation of isoprene. Organic nitrates comprise 30-45% of the NO_y budget during SOAS. Inorganic nitrates were also monitored and showed that during incidents of increased coarse-mode mineral dust, HNO_3 uptake produced nitrate aerosol at rates comparable to that of organic nitrate produced via NO_3 + BVOC.

2

1 Introduction

Secondary Organic Aerosol (SOA), formed from the oxidation of volatile organic compounds (VOCs) by ozone (O_3), hydroxyl radical (OH), or nitrate radical (NO_3), affects visibility as well as regional and global radiative climate forcing (Myhre et al., 2013; Bellouin et al., 2011; Feng and Penner, 2007; Goldstein et al., 2009). Aerosol has been studied as a source for significant risk factors for pulmonary and cardiac disorders (Nel, 2005; Pope and Dockery, 2006). Organic aerosol (OA) contributes a large fraction of the total tropospheric submicron particulate matter (PM, De Gouw, 2005; Heald et al., 2005; Zhang et al., 2007). Biogenic volatile organic compounds (BVOC) are dominant precursors in SOA formation (Goldstein and Galbally, 2007; Spracklen et al., 2011). SOA is a significant fraction of total aerosol mass in the Southeastern United States (SEUS) (predicted to be 80-90% of the organic aerosol load, Ahmadov et al., 2012, Stocker et al., 2013). Understanding the interaction of anthropogenic pollutants with BVOC is vital to improving our understanding of the human impact on SOA formation (Carlton et al., 2010; Spracklen et al., 2011) and the associated radiative forcing of climate change (Stocker et al., 2013).

Nitrogen oxides (NO_x = NO + NO_2), common byproducts of combustion, are linked to aerosol formation in the troposphere via daytime and nighttime oxidation mechanisms (Rollins et al., 2012). Total reactive nitrogen, NO_y, consists of NO_x, as well as NO_x reaction products, including NO_3, HNO_3, HONO, alkyl nitrates, peroxynitrates and other particulate nitrates. Alkyl nitrates produced from oxidation of VOC are related to tropospheric ozone generation (Chameides, 1978) and, via low-volatility products, can lead to formation of SOA (Hallquist et al., 2009). Oxidation of NO_x to nitric acid (HNO_3) can also produce *inorganic* nitrate aerosol via heterogeneous uptake of HNO_3 onto mineral or sea salt aerosols (Vlasenko et al., 2006) and via co-partitioning with ammonia to form semi-volatile NH_4NO_3 (Lee et al., 2008).

Nitrogen oxides are primarily emitted as NO (Nizich et al., 2000; Galloway et al., 2004; Wayne et al., 1991). NO is oxidized to NO_2 and further to the highly reactive NO_3 radical. NO_3 is especially predominant at night when loss via photolysis and NO reaction are at a minimum (Horowitz et al., 2007; von Kuhlmann et al., 2004; Xie et al., 2013).

The formation of NO_3 and the associated N_2O_5 in the atmosphere have been studied in detail (Bertram and Thornton, 2009; Brown and Stutz, 2012; Brown et al., 2011; Wagner et al., 2013). The hydrolysis of N_2O_5 to HNO_3 can be important in the prediction of the tropospheric oxidant burden with respect to the O_3 production, and therefore OH radical production (Dentener and Crutzen, 1993; Evans and Jacob, 2005). However, previous studies in Eastern Texas have found N_2O_5 uptake into aerosols to be relatively low in the southern United States (TexAQS average γ of 0.003) (Brown et al., 2009; Riemer et al., 2009).

NO_3 is an effective nocturnal oxidizer of BVOC (Atkinson and Arey, 2003, 1998; Calogirou et al., 1999; Winer et al., 1984). NO_3 oxidation is especially reactive towards unsaturated, non-aromatic hydrocarbons of which BVOC are major global constituents. NO_3 is less reactive towards aromatic

compounds and saturated hydrocarbons, major compounds of anthropogenic VOCs. Nitrate oxidation of some BVOC compounds, such as β-pinene, lead to rapid production of SOA in laboratory experiments with high yields (Griffin et al., 1999; Jimenez et al., 2009; Zhang et al., 2007; Hallquist et al., 2009; Fry et al., 2011, 2009; Boyd et al., 2015). Analysis of previous field studies have characterized the loss of NO_3 to its major daytime sinks, including reaction with NO and photolysis, as well as its loss to BVOC during both daytime and nighttime (Aldener et al., 2006; Brown et al., 2005).

Nitrogen-containing oxidation products include alkyl nitrates ($RONO_2$), peroxynitrates (RO_2NO_2) and nitric acid (HNO_3) (Brown and Stutz, 2012; Perring et al., 2013), all of which may partition to the aerosol phase and contribute to SOA (via direct reaction or catalysis) (Kroll and Seinfeld, 2008). Ambient concentrations of alkyl nitrates and peroxynitrates can be quantified using laser-induced fluorescence (Day et al., 2002; Rollins et al., 2010) and mass spectrometry methods (Bahreini et al., 2008; Farmer et al., 2010; Beaver et al., 2012; Fry et al., 2013). Ions and acids (i.e. HNO_3) can be quantified using ion chromatography (IC, Makkonen et al., 2012; Trebs et al., 2004) as well as CIMS (Beaver et al., 2012). The combination of these instruments, as well as others discussed below, allow for the determination of a total ambient oxidized nitrogen (NO_y) budget, which enables the interpretation of the importance of nitrogen oxides in SOA formation.

Xu et al. (2015a) have reported that organic aerosol from nitrate radical oxidized monoterpenes are strongly influenced by anthropogenic pollutants and contribute to 19-34% of the total OA content (labeled less-oxidized oxygenated organic aerosols, LO-OOA). Monoterpene oxidation products show a large contribution to LO-OOA year-round (Xu et al., 2015b). Another AMS factor specific to reactive uptake of isoprene oxidation products (e.g. IEPOX), Isoprene-OA, is isolated in the warmer summer months in both urban as well as rural areas across the southeastern United States and contributes 18-36% of summertime OA (Hu et al., 2015; Xu et al., 2015a). LO-OOA is seen predominantly during nighttime hours, implying NO_3 oxidation of monoterpenes, and is strongly correlated specifically with the nitrate functionality in organic nitrates (Xu et al., 2015b). It is suggested that during the summer months, increasing nighttime LO-OOA balances with increasing daytime isoprene-OA to give the observed constant OA concentration over the diurnal cycle.

The 2013 SOAS campaign was a comprehensive field intensive in central Alabama near Centreville (CTR), in which concentrations of oxidants, BVOC and aerosol were measured with a particular focus on understanding the effects of anthropogenic pollution on SOA formation. The site was chosen due to its high biogenic VOC emissions as well as its relatively large distance from anthropogenic pollution (Figure 1). County-level monoterpene emissions across the US shows the CTR site gives a regional representation of monoterpene emissions in the SEUS (Geron et al., 2000). Furthermore, Xu et al. (2015b) show that the CTR site is representative of more-oxidized and less-oxidized oxygenated organic aerosols (MO-OOA and LO-OOA, respectively) loadings across several monitoring stations in the SEUS. Comparison of annual molar emissions in the SEUS (an 8-state region includ-

ing the CTR site) of BVOC (estimated from Geron et al., 2000) to NO_x emissions (from 2011 NEI database) suggest that NO_x is the limiting reagent in BVOC + NO_3 reactions throughout the region.

Alabama is home to a number of power plant facilities that are large point sources of NO_x capable of being carried long distances. Alabama's non-interstate roadways also have large emissions of NO_x, though a majority of the emissions come from urban areas. Although the NO_x emissions have been steadily dropping since 1998, they are still substantial (2.70 million tons in reported for SEUS in 1999 to 1.75 million tons in 2008, Blanchard et al., 2013). Frequent controlled biomass burning events (crop burning, Crutzen and Andreae, 1990), as well as vehicular sources (Dallmann et al., 2012) also contribute to local NO_x emissions and PM concentrations (a full analysis of contributions can be found at the EPA National Emissions Inventory, http://www.epa.gov/ttn/chief /net/2011inventory.html).

In the present study, we investigate the production of SOA species from NO_3 reaction with monoterpenes. NO_3 loss to BVOC is calculated and compared to AMS and TD-LIF measurements of aerosol organic nitrates, as well as individual product nitrates measured by CIMS. We compare this NO_3 loss to BVOC to an alternate fate of NO_x, heterogeneous HNO_3 uptake to produce inorganic nitrate aerosol, which is considered in detail in a companion paper (Allen et al., 2015). These two pathways from NO_x to nitrate aerosol shown in Scheme 1 alternated dominance during SOAS.

2 Experimental

Measurements for the SOAS campaign took place near the Talladega National Forest, 6 miles southwest of Brent, AL (32.9029 N, 87.2497 W), from June 1 - July 15, 2013. The forest covers 157,000 acres to the northwest and southeast of Centerville, AL. Figure 1 shows a map of the site location as well as nearby point sources of anthropogenic NO_x and SO_2. The site is in a rural area representative of the transitional nature between the lower coastal plain and Appalachian highlands (Das and Aneja, 2003). Wind direction varied during SOAS allowing for periods of urban influence from sources of anthropogenic emissions located near the sampling site, including the cities of Montgomery, Birmingham, Mobile and Tuscaloosa (Hidy et al., 2014). The closest large anthropogenic NO_x emission point sources are the Alabama Power Company Gaston Plant located near Birmingham and the Green County Power Plant southwest of Tuscaloosa (EPA Air Markets Program 2013).

Two cavity ringdown spectrometers (CRDS) were used to determine ambient mixing ratios of NO_x, O_3, NO_y, NO_3 and N_2O_5 (Wild et al., 2014; Wagner et al., 2011). CRDS is a high sensitivity optical absorption method based on the decay time constant for light from an optical cavity composed of two high reflectivity mirrors. NO_2 is measured using its optical absorption at 405 nm in one channel, and O_3, NO and total NO_y are quantitatively converted to NO_2 and measured simultaneously by 405 nm absorption on three additional channels. NO_3 is measured at its characteristic strong absorption band at 662 nm. N_2O_5 is quantitatively converted to NO_3 by thermal dissociation

and detected in a second 662 nm channel with a detection limit of 1 pptv (30 s, 2 σ) for NO_3 and 1.2 pptv (30 s, 2 σ) for N_2O_5 (Dubé et al., 2006; Wagner et al., 2011).

Thermal Dissociation Laser-Induced Fluorescence (TD-LIF, $PM_{2.5}$ size-cut) (Day et al., 2002; Farmer et al., 2010; Rollins et al., 2010) was used to measure total alkyl nitrates (ΣANs), total peroxy nitrates (ΣPNs) and aerosol phase ΣANs (Rollins et al., 2012). High-resolution time-of-flight aerosol mass spectrometry (HR-ToF-AMS, hereafter AMS, DeCarlo et al., 2006; Canagaratna et al., 2004, PM_1 size-cut) was used to measure submicron organic and inorganic nitrate aerosol composition using the nitrate separation method described in Fry et al. (2013). Organic nitrates in the particle phase ($pRONO_2$) decompose prior to ionization on the AMS vaporizer to NO_2^+ organic fragments, hence $pRONO_2$ cannot be quantified directly from AMS data. The contribution of $pRONO_2$ to total particulate nitrate was calculated using the method first discussed in Fry et al. (2013) and is briefly summarized here. This method relies on the different fragmentation patterns observed in the AMS for organic nitrates vs NH_4NO_3, specifically the ratio of the ions NO_2^+ to NO^+. Since this ratio depends on mass spectrometer tuning, vaporizer settings and history, Fry and coauthors proposed to interpret the field ratio of these ions in relation to the one recorded for NH_4NO_3 (which is done routinely during in-field calibrations of the instrument). Using such normalized ratios, most field and chamber observations of pure organic nitrates are consistent with $(NO_2^+/NO^+)/((NO_2^+/NO^+)ref$ of 1/2.25 (Farmer et al., 2010) to 1/3 (Fry et al., 2009) of the calibration ratio. The data reported here was calculated using the 1/2.25 ratio derived from Farmer et al. (2010) and used in Fry et al. (2013), interpolating linearly between pure ammonium nitrate and organic nitrate. It should be noted that a) the relative ionization efficiency (RIE) for both types of nitrate is assumed to be the same (since similar neutrals are produced) and b) that the organic part of the molecule will be quantified as OA in the AMS. Therefore, while only equivalent NO_2 $pRONO_2$ can be reported from AMS measurements, this makes the technique well suited for comparison with the TD-LIF method. These measurements correlate well to one another, but the magnitudes differ by a factor of approximately 2-4 for unknown reasons, with TD-LIF being larger than AMS (see Supplemental Information).

Two chemical ionization mass spectrometers (Caltech's cTOF-CIMS and University of Washington's HR-ToF-CIMS, hereafter both referred to as CIT-CIMS and UW-CIMS respectively, Bertram et al., 2011; Yatavelli et al., 2012; Lee et al., 2014; Nguyen et al., 2015) were used to identify specific organic nitrate product ions, specifically monoterpene (Eddingsaas et al., 2012) and isoprene products (Crounse et al., 2013, 2006; Beaver et al., 2012). The CIT-CIMS measured only gas phase products (Beaver et al., 2012; Nguyen et al., 2015) while the UW-CIMS employed a Filter Inlet for Gas and Aerosol (FIGAERO) to separate aerosol and gas species (Lopez-Hilfiker et al., 2014; Lee et al., 2014, 2015). Both spectrometers are capable of resolving ions with different elemental formulae at common nominal m/z.

On-line cryostat-Gas Chromatography-Mass Spectrometer (GC-MS) was used to measure mixing ratios of gas phase BVOC species (Goldan et al., 2004; Gilman et al., 2010). BVOC emissions at

the CTR site are dominated by isoprene, α-pinene, β-pinene, and limonene (Supplemental Figure S4, Stroud et al., 2002; Goldan et al., 1995). Surface area concentration was calculated from number distribution measurements of a hygroscopicity scanning mobility particle sizer (SMPS) and optical particle sizer (OPS) similar to a Dry-Ambient Aerosol Size Spectrometer (Stanier et al., 2004). Boundary layer height was measured using a CHM 15k-Nimbus and method employs photon counting of back-scattered pulse of near-IR light (1064 nm) via LIDAR principle. A Metrohm Monitor for Aerosols and Gases in Ambient Air (MARGA, Makkonen et al., 2012; Trebs et al., 2004; Allen et al., 2015, $PM_{2.5}$ size-cut), which combines a wet-rotating denuder and steam jet aerosol collector inlet with positive and negative ion chromatography, measured inorganic ion concentrations at 1-hour time resolution in both the aerosol- and gas-phases.

Site infrastructure consisted of a 65-foot tower, with the top platform set above the canopy height for sampling to prevent bias between measurements, and seven trailers located in a field 90 m south of the tower. The tower instruments used for this analysis consisted of the two CRDS, CIT-CIMS, TD-LIF and a cryostat GC-MS. The field trailers contained the AMS, SMPS, APS, UW-CIMS and MARGA.

3 Results

3.1 Organic NO_x sink: NO_3 + BVOC production of organic nitrate SOA

During the SOAS campaign, we monitored reactant and product species indicative of NO_3 + BVOC, which may partition into the aerosol phase and consequently serve as a source of first generation SOA. NO_3 reaction with biogenic alkenes forms organic nitrates (R1).

$$NO_3 + BVOC \rightarrow RONO_2 + \text{other products} \tag{R1}$$

NO_3 and N_2O_5 (which exists in equilibrium with NO_2 + NO_3) in the region were consistently low during the campaign. The resulting NO_3 mixing ratio was below the detection limit of the cavity ringdown instrument (1 pptv) for the entire campaign. Calculated steady-state N_2O_5 was validated against observed measurements (see below) and NO_3 predicted from the steady-state approximation was used for all calculations involving NO_3 radical mixing ratios. Using the rate constant for NO_2 + O_3 (Table 1), the production rate of the nitrate radical ($P(NO_3)$) is given by:

$$P(NO_3) = k_{O_3 + NO_2}[O_3][NO_2] \tag{1}$$

The calculated loss rate of NO_3, $\tau(NO_3)$, to reactions with individual BVOC, NO and photolysis. (j_{NO_3}, modeled for clear sky from MCM, (Saunders et al., 2003)) is

$$\tau(NO_3) = \frac{1}{\left(\sum_i k_{NO_3 + BVOC_i}[BVOC]_i + k_{NO_3 + NO}[NO] + j_{NO_3}\right)} \tag{2}$$

7

195 j_{NO_3} values were calculated from solar zenith angles and NO_3 photolysis rates (Saunders et al., 2003). The values were then adjusted for cloud cover by taking measured solar radiation values (Atmospheric Research and Analysis, Inc., W/m^2) and normalizing their peak values to those of the modeled photolysis data. Peak modeled j_{NO_3} values were $0.175 \ s^{-1}$ for clear sky at the daily solar maximum. After normalizing, typical values of j_{NO_3} were $0.110 \ s^{-1}$ during daytime.

200 Using equations 1 & 2, a steady-state predicted NO_3 mixing ratio ($NO_{3,SS}$) can be calculated:

$$[NO_3]_{SS} = \frac{P(NO_3)}{\tau(NO_3)^{-1}} \tag{3}$$

$NO_{3,SS}$ can then be used to calculate steady-state predicted N_2O_5 from the N_2O_5 equilibrium (Table 1) and measured NO_2

$$[N_2O_5]_{SS} = K_{eq}[NO_2][NO_3]_{SS} \tag{4}$$

205 where K_{eq} is $2.7x10^{-27}exp^{(11000/T)}cm^3$ molecule^{-1} s^{-1} (Sander et al., 2011, see Table 1). Comparison of the predicted N_2O_5 to the measured N_2O_5 mixing ratios for the campaign demonstrates that both timing and magnitude of predicted N_2O_5 peaks match observations (Figure S1). Predicted steady-state N_2O_5 tracked observations when the latter were available and propagation of the error of calculated N_2O_5 shows peak measured values fall within uncertainty bounds of the predicted

210 (Figure S2a); therefore, $NO_{3,SS}$ is hereafter used as the best estimate of NO_3 to calculate production rates of BVOC-nitrate products. $NO_{3,SS}$ peaks at 1.4 ppt $\pm$ 0.4 ppt. Propagation of errors in rate constants in the $NO_{3,SS}$ calculation (Figure S2b) shows that the error spans or is close to a mixing ratio of 0 for NO_3 during the entire campaign when data was available. Correlation of measured N_2O_5 vs predicted N_2O_5 shows that during periods of high N_2O_5, we overestimate the concentration by a

215 factor of two (Figure S1). Furthermore, propagation of error in the $NO_{3,SS}$ calculation (Figure S2b) shows that the error encompasses the measured NO_3 during the entire campaign when data was available, showing that predicted $NO_{3,SS}$ is consistent with the lack of detection of NO_3 by CRDS.

A substantial fraction (30-45%) of the NO_y budget is comprised of organic nitrates (ΣANs + ΣPNs, Figure S3). Measurements of gas phase and aerosol phase alkyl nitrates show that a sub-

220 stantial fraction of the organic nitrates are in the aerosol phase (30% when aerosol phase AMS is compared to TD-LIF total ΣANs vs 80% when comparing aerosol phase ΣANs to TD-LIF total ΣANs at 5 am CDT) when total ΣANs concentration builds up (Figures 2 & 3). The average diurnal cycle shown in Figure 3 also shows that TD-LIF measured ΣANs are almost completely in the aerosol phase at night, but only about 50% in the aerosol phase during the day. During peaks in

225 $NO_{3,SS}$, we see corresponding spikes in the ΣANs concentrations as well as organic nitrate concentration from AMS, all of which occur during nighttime periods (Figure 2). This is consistent with organic nitrates formed by NO_3 + BVOC rapidly partitioning into the aerosol phase.

BVOC measurements show large mixing ratios of isoprene throughout the entire campaign (daytime peaks above 8 ppb), followed by α- and β-pinene (peak nighttime mixing ratios of 0.5-1 ppb,

Figure S4). Using the measured mixing ratios of VOC, and their reaction rates with NO_3, predicted NO_3 losses are calculated and compared to organic nitrate aerosol. Figure 4 shows the diurnally averaged NO_3 losses for the entire campaign period (June 1 - July 15, 2013). Daytime losses include photolysis and reaction with NO. Approximately half the daytime losses are due to reaction of NO_3 with BVOC (Note, this does not necessarily imply that NO_3 reaction is a substantial loss process *from the perspective of BVOC*; during the day, $P(HO_x)$ exceeds $P(NO_3)$ by a factor of 10-70 at SOAS, so OH will typically dominate.) However, from the standpoint of NO_3 lifetime, previous forest campaigns have assumed NO_3 + monoterpene reactions to be important only during the night and that photolysis and NO losses were the dominant NO_3 sinks during the day (Geyer et al., 2001; Warneke et al., 2004). In this study, we predict significant losses of NO_3 to isoprene and monoterpenes during daylight hours.

To assess heterogeneous losses of N_2O_5 to particles, an uptake rate coefficient of N_2O_5 into deliquesced aerosols is estimated using PM surface area ($S_A, nm^2/cm^3$), the molecular speed of N_2O_5 ($\bar{c}$, m/s) and the uptake coefficient ($\gamma_{N_2O_5}$).

$$k_{het} = \frac{1}{4} \times \gamma_{N_2O_5} \times \bar{c}_{N_2O_5} \times S_A \tag{5}$$

Conditions of high relative humidity in the SEUS necessitated a higher γ of 0.02 as the uptake coefficient (Bertram and Thornton, 2009; Crowley et al., 2011) which represents an upper limit from previous field studies (Brown et al., 2009, Brown et al., 2006). We predict heterogeneous N_2O_5 uptake to be very small over the campaign despite high relative humidity. When $PM_{2.5}$ concentration was at its highest in mid-July, the calculated uptake rate coefficient was calculated at 1.6×10^{-3} s^{-1} in mid July, representing less than 1% of the loss of NO_3.

3.1.1 Calculation of NO_3 loss to BVOC

Using literature NO_3 + BVOC rate coefficients and calculated $NO_{3,SS}$, we calculate instantaneous NO_3 loss rates (($NO_{3,loss})_{inst}$) for the campaign.

$$(NO_{3,loss})_{inst} = \sum_i k_{NO_3+VOC_i} [VOC]_i [NO_3]_{SS} \tag{6}$$

BVOC mixing ratios from GC-MS and rate constants shown in Table 1 were used to calculate the time-integrated nitrate loss to reactions with BVOC.

$$(NO_{3,loss})_{integ} = \sum_{i,t} (NO_{3,loss})_{inst,i} \times \Delta t \tag{7}$$

Specifically, time loss of NO_3 radical to reaction with BVOC (($NO_{3,loss})_{integ}$) were calculated during periods of increasing $RONO_2$ concentrations as monitored by CIMS or aerosol phase $RONO_2$ monitored by AMS or TD-LIF during SOAS. The beginning and end of the buildup periods were chosen as the approximate trough and peak values for the individual analyses (CIMS, AMS and TD-LIF). This buildup of aerosol $RONO_2$ was only observed after sunset with one buildup event

9

per night. The boundary layer during night hours is relatively stable, such that NO_x and BVOC measurements can be considered an area-wide average and this simple box model can be used to calculate $(NO_{3,loss})_{integ}$ (6, 7).

Under the assumption of a constant nighttime boundary layer height and an approximately uniform, area wide source that limits the time rate of change due to horizontal advection (i.e., a nighttime box), the time integrals of $RONO_2$ produced provide estimates of the evolution of $RONO_2$ concentrations at night (this assumption was verified using CO to minimize first order effects of dilution from changes in the boundary layer (Blanchard et al., 2011)). Time periods of CIMS $RONO_2$ or aerosol buildup were chosen to determine time intervals for calculation of $(NO_{3,loss})_{integ}$ when data was available.

$(NO_{3,loss})_{integ}$ is the calculated time integral of the reaction products of NO_3 with individual or combined mixing ratios of BVOC and Δt is the time step between each calculated value of $(NO_{3,loss})_{inst,i}$. Data are averaged to 30 minute increments, a time step sufficient to resolve the observed rate of change. Figure 5 shows an example of the resulting calculated integrated NO_3 losses from (7) to both isoprene and summed monoterpenes. These nightly loss values are correlated with organic nitrate gas- and aerosol-phase measurements and linear fits and correlation coefficients were calculated to aid in the interpretation of gas- and aerosol-phase organic nitrate formation. Note that these peak times occur during nighttime hours when the boundary layer is shallow (Figure S5).

3.1.2 Implied organic nitrate and SOA yields

The correlation slopes in Figure 6 are in $ppb_{aerosol}/ppb_{(NO_{3,loss})_{integ}}$ and indicate the average molar organic nitrate aerosol yield. The AMS and TD-LIF measurements of aerosol phase organic nitrates suggest a molar yield of 23 and 44%, respectively (Figure 6). This calculation uses all available data from each instrument and assumes no other processes are taking place. We note that without knowledge of the average molecular weight of the aerosol organic nitrate, only molar yield estimates are possible. Several chamber studies have measured organic nitrate yields from NO_3 oxidation of individual terpenes: Spittler et al. (2006) and Fry et al. (2014) both found 10-15% total organic nitrate (ON) yield for α-pinene (entirely in the gas phase); Fry et al. (2009) found 45% total ON yield for β-pinene under humid conditions, Fry et al. (2014) found 22% under dry conditions, and Boyd et al. (2015) found aerosol organic nitrate to comprise 45-74% of OA produced from NO_3 + β-pinene; and Fry et al. (2011) found 30% total ON yield while Fry et al. (2014) found 54% for limonene. A mix of these chamber organic nitrate yields are consistent with the observed molar yield range reported here, which uses only NO_3 losses to monoterpenes.

To derive an estimated SOA mass yield from these correlations, we propose the following rough calculation. Conversion of the reported molar yield to an SOA mass yield requires assuming 1:1 reaction stoichiometry of NO_3 with monoterpenes (MW = 136 g mol^{-1}) and estimating the average molecular weight (250 g mol^{-1}) of the condensing organic nitrates. Using the range of molar yields

determined here (23-44%), this conversion gives an SOA mass yield range from 42% to 81%. These apparent aggregated yields of SOA from NO_3 + monoterpene are higher than one might expect from laboratory-based yields from individual monoterpenes, particularly since $NO_3 + \alpha$-pinene SOA yields are essentially zero (Fry et al., 2014; Hallquist et al., 1999; Spittler et al., 2006) and α-pinene is a dominant monoterpene in this region. For β-pinene, Fry et al. (2009), Fry et al. (2014) and Boyd et al. (2015) found SOA mass yields in the 30-50% range at relevant loading and relative humidity, and Fry et al. (2011) and Fry et al. (2014) found a limonene SOA yield of 25-57%. Because the actual average molecular weight of the condensing species is unknown (we do not include sesquiterpene oxidation products and higher molecular weight BVOC products as reported by Lee et al. (2015), with which we would calculate larger SOA mass yields), this comparison is not straightforward, but it appears that the aggregate SOA yield suggests higher ultimate SOA mass yields than simple chamber experiments dictate, perhaps suggesting that post-first generation products create more condensable species.

Since nitrate product buildup occurs over multiple hours (Figure 5), the rapid particulate organic nitrate losses (timescale of 2-4 hours) found by researchers at the University of Washington are a lower limit. This also does not take into account heterogeneous hydrolysis (Boyd et al., 2015; Cole-Filipiak et al., 2010; Liu et al., 2012), photolysis (Epstein et al., 2014; Müller et al., 2014), or reaction with the hydroxyl radical (OH) (Lee et al., 2011). Because understanding of these nitrate loss processes is poor, a quantitative estimate of how this would affect derived molar yields would be premature.

Finally, because this yield is based on total ambient monoterpene concentrations, it incorporates nitrate radical loss to α-pinene, which is known to produce very modest yields of SOA (0-10%) from NO_3 reaction (Fry et al., 2014; Spittler et al., 2006). This suggests effective overall SOA yields from other BVOC must be large.

3.1.3 Organic Nitrate Product Analysis

Observations of $NO_{3,SS}$ compared to TD-LIF and AMS (Figure 2) suggest aerosol organic nitrates are dominated by nighttime NO_3 + BVOC, rather than other known nitrate-producing reactions (e.g. RO_2 + NO), which would dominate during the daytime and would not coincide with peaks in $[NO_3]$.

Researchers at University of Washington describe the observation of particle phase C_{10} organic nitrate concentrations peaking at night during SOAS (Lee et al., 2015), consistent with high SOA yield from NO_3 + monoterpenes. Observed C_{10} organic nitrates include many highly oxidized molecules, suggesting that substantial additional oxidation beyond the first-generation hydroxynitrates occurs (Lee et al., 2015). Specific first generation monoterpene organic nitrate compounds were identified and measured in the gas- and aerosol-phases (Lopez-Hilfiker et al., 2014; Beaver et al., 2012). Using the $(NO_{3,loss})_{integ}$ calculations, another correlation analysis is conducted to identify key gas- and aerosol-phase products of NO_3 oxidation. Observed buildups in gas- and aerosol-phase organic

nitrate concentrations from each CIMS are scattered against predicted $(NO_{3,loss})_{integ}$ to monoterpenes (Figure 7). The generally good correlations suggest that all of the molecular formulae shown here have contributions from NO_3 oxidation. Comparisons of observed R^2 values and slopes for each of these correlation plots may then provide some mechanistic insight. For example, the species with larger R^2 ($C_{10}H_{17}NO_5$) may indicate a greater contribution to these species from NO_3 radical chemistry. If we assume the same sensitivity across phases in the cases where the same species is observed (Figure 7a/b and d/e), we can estimate the relative amount in each phase by the ratio of the slopes. This would suggest that $C_{10}H_{15}NO_5$ partitions more to the particle phase than $C_{10}H_{17}NO_5$.

Although the gas phase monoterpene nitrate product correlations display substantial scatter, likely due to their multiple possible sources and rapid partitioning to the aerosol phase, we can use the calibrated mixing ratios measured by the CIT-CIMS to calculate approximate lower limit molar yields for $C_{10}H_{15}NO_5$ (0.4%), $C_{10}H_{17}NO_5$ (3%), and $C_{10}H_{17}NO_4$ (3%) from NO_3, based on the slope of correlations shown in panels c, f and h. We estimate these to be lower limits, because no losses of these species during the period of buildup is taken into account in this correlation analysis.

The median particulate fraction of $C_5H_9NO_5$ (particle phase/total) observed by the UW-CIMS was less than 1%, and $C_5H_9NO_{5(p)}$ comprised less than 1% of total particulate organic nitrate (Lee et al., 2015). Those C_5 species that are observed in the particle phase constitute less than 12% of total particulate organic nitrate mass (as measured by the UW-CIMS, Lee et al., 2015 Supplemental Information), and are more highly oxidized molecules, inconsistent with first-generation NO_3 + isoprene products. This suggests that most (especially first-generation) isoprene nitrate products remain in the gas phase. The correlation of gas phase first-generation isoprene nitrate concentrations with NO_3 loss again provides evidence about the oxidative sources of these molecules (Figure 8). $C_5H_9NO_5$ (panels a and b) shows the strongest correlation with $(NO_{3,loss})_{integ}$ to isoprene among all the individual molecules (R^2 = 0.54 for UW and 0.70 for CIT), suggesting that this compound is a product of NO_3 oxidation. The better correlations of these C_5 species than observed in Figure 7 may be due to slower gas phase losses of organic nitrates relative to the semi-volatile C_{10} species. Using the calibrated mixing ratios from CIT for $C_5H_9NO_5$, we calculate an approximate lower limit molar yield of 7%. The $C_5H_9NO_4$ and $C_4H_9NO_5$ isoprene products (panels c and d) show poorer correlation with $(NO_{3,loss})_{integ}$ to isoprene (R^2 =0.11 and 0.35, respectively), suggesting that these products are not (exclusively) a NO_3 + isoprene product, and may instead be a photochemically or ozonolysis produced organic nitrate, via RO_2 +NO.

We note that the two CIMS for which data is shown in Figures 7 and 8 were located at different heights: the CIT-CIMS was atop the 20 meter tower, collocated with the measurements used to determine $[NO_3]_{ss}$, while the UW-CIMS measured at ground level. Particularly at nighttime, it is possible that this lower 20 meters of the nocturnal surface layer can become stratified, so some scatter and differences in correlations between instruments arising from this occasional stratification are not unexpected.

3.2 Comparison to Inorganic NO_x sink: NO_3^- aerosol production from heterogeneous uptake of HNO_3

Partitioning of semivolatile ammonium nitrate into aerosol represented a small fraction of aerosol contribution throughout the campaign based on AMS and MARGA data (Allen et al., 2015). A more important route of NO_x conversion to nitrate aerosol occurred via HNO_3 heterogeneous reaction on the surface of dust or sea salt particles (Scheme 1). This process, which was observed to be especially important during periods of high mineral or sea salt supermicron aerosol concentrations, is described in detail in a companion paper (Allen et al., 2015). Briefly, we observe that while concentrations of organic and inorganic nitrate aerosol are generally comparable (Figure S3 and Figure 3), the inorganic nitrate is more episodic in nature. Periods of highest NO_3^- concentration as measured by the MARGA were observed during two multi-day coarse-mode dust events, from June 9 to 15 and June 23 to 30, while organic nitrates have a more regular diurnal pattern indicative of production from locally-available reactants, with most of the organic nitrate present in the condensed phase (Figure 3).

In order to estimate the fluxes of NO_x loss to aerosol via the two pathways shown in Scheme 1, we calculate the reactive losses of NO_2 to organic nitrate (limiting rate is taken to be $\sum_i k_i[NO_3][BVOC]_i$, with the included terpenes α-pinene, β-pinene, limonene and camphene) and to inorganic nitrate via heterogeneous HNO_3 uptake (Allen et al., 2015). A substantial fraction of the suface area is in the transition regime, so HNO_3 uptake is reduced due to diffusion limitations. To account for this, a Fuchs-Sutugin correction is applied (Seinfeld and Pandis, 2006):

$$\text{Rate} = \sum^{R_p} \frac{S_a}{R_p} D_g \left(\frac{0.75\alpha(1+Kn)}{Kn^2 + Kn + 0.283Kn\alpha + 0.75\alpha} \right) [HNO_3] \tag{8}$$

with S_a is surface area, R_p is the radius, D_g is the diffusivity of HNO_3 in air (0.118 cm^2 s^{-1}) and α is estimated at 0.1 for an upper limit.

Since we have seen that the organic nitrates are present predominantly in the condensed phase, we take this comparison to be the relative rate of production of organic nitrate aerosol vs. inorganic nitrate aerosol (Figure 9), and we see that over the summer campaign, the rates are comparable in magnitude, but peak at different times. This analysis suggests that substantial nitrate aerosol (peak values of 1 μg m^{-3}hr^{-1}, with average rates 0.1 μg m^{-3}hr^{-1} for both inorganic and organic nitrate rates) is produced in the SEUS by both inorganic and organic routes (depicted in Scheme 1), converting local NO_x pollution to particulate matter. We note that this calculation accounts only for the production rates of these two types of nitrate aerosol and does not account for subsequent chemistry that may deplete one faster than the other; hence, relative mass concentrations are not necessarily expected to correlate directly to these relative production rates.

13

3.3 Implications of NO_3 oxidation on SOA formation in the SEUS

The importance of the NO_3 + BVOC reaction SOA has only recently been recognized (Beaver et al., 2012; Fry et al., 2013; Rollins et al., 2012). Pye et al. (2010) showed that including NO_3 radical oxidation increased predicted SOA yields from terpenes by 100% and total aerosol concentrations by 30% (Pye et al., 2010). The results of this study underscore the importance of NO_3 in SOA formation. Measured aerosol organic nitrate concentrations are correlated with the reaction of NO_3 with BVOC. This pathway is especially important before sunrise when competing oxidants (O_3 and OH) are at a minimum.

We can estimate the contribution of this NO_3 + BVOC mechanism to total particulate matter using the 2011 NEI data for the states included in the 2004 Southern Appalachian Mountain Initiative study (SAMI, Odman et al., 2004): Kentucky, Virginia, West Virginia, North Carolina, South Carolina, Tennessee, Alabama and Georgia (http://www.epa.gov/ttn/chief/net/2011inventory.html). In this 8-state region, the NEI reported emissions of 2.3 Tg yr^{-1} (2.5×10^6 tons yr^{-1}) of nitrogen oxides and 0.8 Tg yr^{-1} (9×10^5 tons yr^{-1}) of $PM_{2.5}$ in 2011. We can estimate the fraction of the NO_x emitted that is converted to PM using several assumptions. NO_2 is estimated to contribute 50% of the NO_y budget (Figure S3), so we multiply the NO_x emission by 0.5 to account for half of the instantaneous NO_x residing in the atmosphere as other NO_y species at any given time. An average lifetime of 16 hours for O_3 + NO_2 reaction was calculated ($1/k[O_3]$) and, with an average nighttime length of 9 hours, we estimate about 55% of NO_2 is converted to NO_3 overnight. Using the average molar organic nitrate aerosol yield of 30% determined in this study and an estimated molecular weight of 250 g mol^{-1} for oxidized product (terpene hydoxynitrate with two additional oxygen functional groups, Draper et al., 2015), we convert from molar yield to mass yield of organic nitrate aerosol. This assumes that NO_x is the limiting reagent for SOA production from this chemistry; as noted in the introduction, comparison of regional NO_x and BVOC emissions rates supports this assumption. Finally, using the summed NEI NO_x emissions data for the SAMI states, we calculate a source estimate of 0.6 Tg yr^{-1} of NO_3-oxidized aerosol. Adding this to the NEI primary $PM_{2.5}$ emissions estimate of 0.8 Tg yr^{-1} gives a total 1.4 Tg yr^{-1}, showing that NO_3 initiated SOA formation would contribute a substantial additional source of $PM_{2.5}$ regionally, nearly doubling primary emissions. Model calculations by Odman et al. (2004) for the SAMI states estimated 1 Tg yr^{-1} of total $PM_{2.5}$ in 2010, including primary and secondary sources. Their modeled $PM_{2.5}$ emissions are lower than our rough estimate here, despite the fact that actual 2010 NO_x emissions were 2.3 Tg yr^{-1} rather than the 3 Tg yr^{-1} projected at that time. Hence, despite successful reduction of regional NO_x emissions (Blanchard et al., 2013), this work suggests that secondary $PM_{2.5}$ production from NO_3 oxidation of regionally abundant BVOCs remains a substantial anthropogenic source of pollution in the SEUS.

4 Conclusions

The contribution of NO_3 + BVOC to SOA formation is found to be substantial in the terpene-rich SEUS. An estimated 23-44% of nitrate radical lost to reaction with monoterpenes becomes aerosol phase organic nitrate. Predicted nitrate losses to isoprene and to monoterpenes are calculated from the steady-state nitrate and BVOC mixing ratios and then time integrated during evenings and nights as $RONO_2$ aerosol builds up. Correlation plots of AMS, TD-LIF, and CIMS measurements of gas- and aerosol-phase organic nitrates against predicted nitrate losses to monoterpenes indicate that NO_3 + monoterpenes contribute substantially to observed nitrate aerosol. Two specific C_{10} structures measured by CIMS are shown to be NO_3 radical products by their good correlation with cumulative $(NO_{3,loss})_{integ}$; their semi-volatile nature leads to their variable partitioning between gas- and aerosol-phase. Calibrated gas phase mixing ratios of selected organic nitrates allow estimation of lower limit molar yields of $C_5H_9NO_5$, $C_{10}H_{17}NO_4$, $C_{10}H_{17}NO_5$ from NO_3 reactions (7%, 3%, and 3% respectively). The fact that these molar yields of monoterpene nitrates are substantially lower that the aggregated aerosol phase organic nitrate yield may suggest that further chemical evolution is responsible for the large SOA yields from these reactions, consistent with Lee et al. (2015). The NO_3 + BVOC source of nitrate aerosol is comparable in magnitude to inorganic nitrate aerosol formation, and is observed to be a substantial contribution to regional $PM_{2.5}$.

Table 1. NO_3 kinetic rate constants and equilibrium constants used to determine losses.

Reaction	A	E_a/R*	B**	k(298 K)	Source
$O_3 + NO_2 \rightarrow O_2 + NO_3$	1.2×10^{-13}	2450			Sander et al. (2011)
$NO_3 + NO_2 \rightleftharpoons N_2O_5$	2.7×10^{-27}		11000		Sander et al. (2011)
$NO + NO_3 \rightarrow 2NO_2$	1.5×10^{-11}	-170			Sander et al. (2011)
Isoprene + $NO_3 \rightarrow$ Products	3.03×10^{-12}	446			Calvert et al. (2000)
α-pinene + $NO_3 \rightarrow$ Products	1.19×10^{-12}	-490			Calvert et al. (2000)
β-pinene + $NO_3 \rightarrow$ Products				2.51×10^{-12}	Calvert et al. (2000)
Camphene + $NO_3 \rightarrow$ Products				6.6×10^{-13}	Calvert et al. (2000)
Myrcene + $NO_3 \rightarrow$ Products				1.1×10^{-11}	Calvert et al. (2000)
Limonene + $NO_3 \rightarrow$ Products				1.22×10^{-11}	Calvert et al. (2000)

* Reaction rate constants are reported as: k(T) = A $e^{-(E_a/R)/T}$, in units of $(cm^3 \ molecule^{-1} \ s^{-1})$

** Equilibrium constants are reported as: K_{eq} = A $e^{B/T}$, in units of $(cm^3 \ molecule^{-1})$

Scheme 1 Generalized reaction fate for NO_2 in the troposphere. Oxidation of NO_2 from atmospheric oxidants leads to two possible paths.
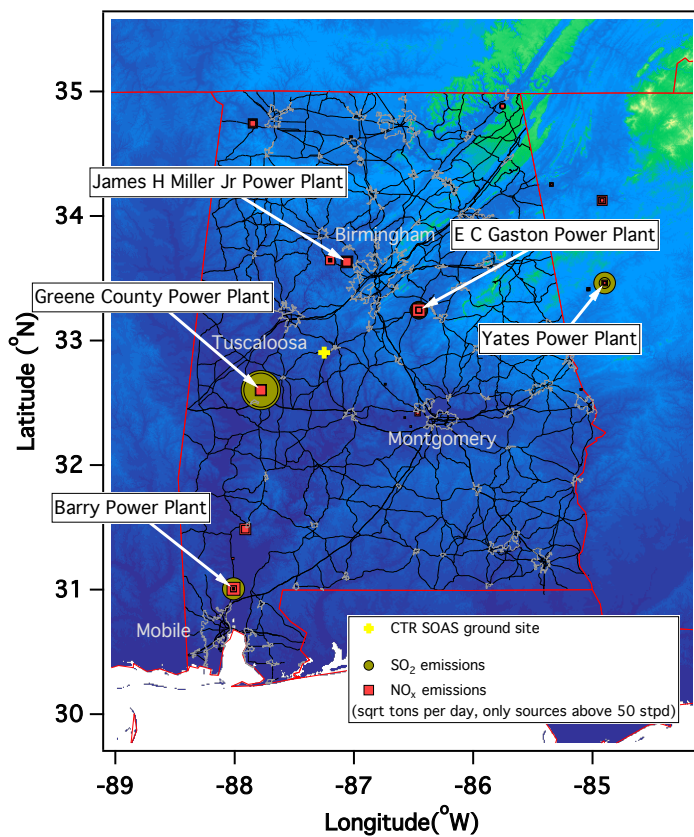
$$NO_2 \xrightarrow{O_3} NO_3 \xrightarrow{BVOC} \text{organonitrates} \longleftrightarrow \textcolor{blue}{\text{organonitrate aerosol}}$$

$$NO_2 \xrightarrow{OH} HNO_3 \xrightarrow[\text{surface}]{\text{aerosol}} \textcolor{red}{\text{inorganic nitrates}}$$
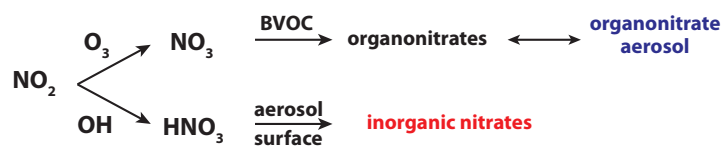
Figure 1. Map of Alabama with SO_2 and NO_x emissions point sources shown, as well as major roadways (black) . Centreville is located in Central Alabama about 55 miles SSW of Birmingham, AL. Major highways, city limits and major contributors to emissions are referenced for Alabama. The size of the emission markers depicts the relative concentrations of the pollutants according to the 2013 EPA Air Markets Program. For reference, the Alabama Power Company Gaston Plant emits 19.52 kg hr^{-1} SO_2 and 6.43 kg hr^{-1} NO_x.

18
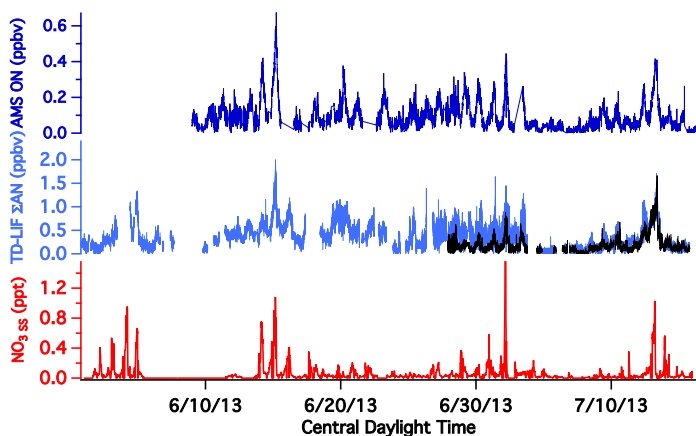
Figure 2. Nitrate radical concentration estimated by the steady-state approximation (red trace) shows several instances where peaks in NO_3 concentration correspond to times of ΣAN (gaseous+aerosol) buildup (light blue trace) from TD-LIF and particle phase organic nitrate from AMS (dark blue). The black overlay in TD-LIF ΣANs is the aerosol phase measurement of ΣANs and qualitatively shows that, when data is available, a large portion of the organic nitrates appear to be in the aerosol phase.
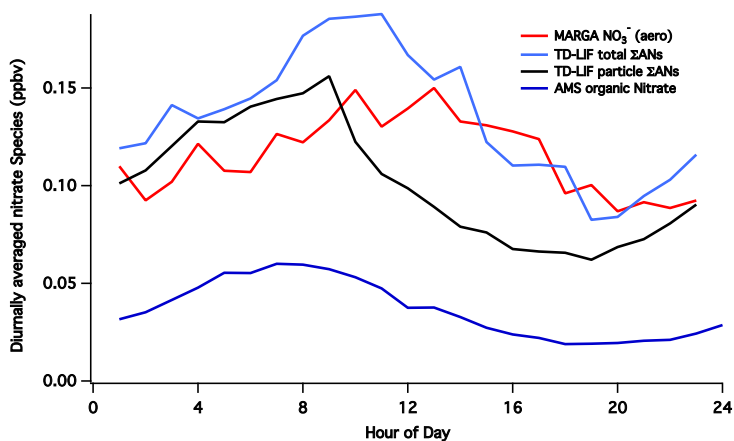

Figure 3. Diurnally averaged organic and inorganic nitrates show organic nitrates peaking in the early morning and inorganic nitrates peaking midday. Note the AMS had a PM_1 size-cut, while MARGA and TD-LIF had a $PM_{2.5}$ size-cut. See text and supplemental information for more details on this comparison.

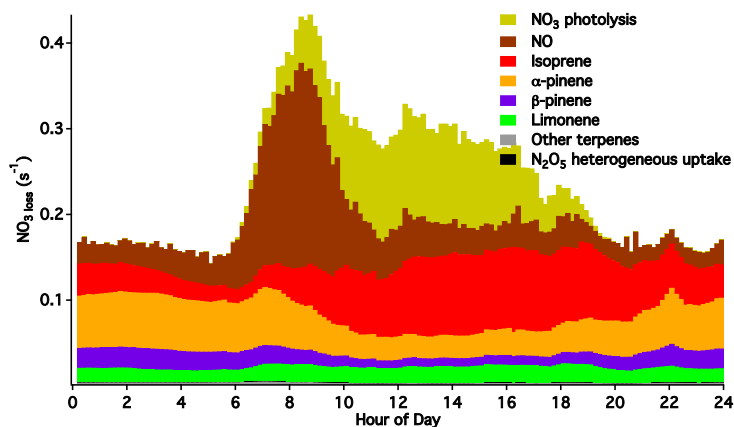**Figure 4.** Average diurnal profile of NO_3/N_2O_5 losses June 1 - July 15, 2013. NO and photolysis losses peak during the daytime (in fact, nighttime NO_3 + NO loss is likely zero, and even [NO] below the instrument detection limits would cause the non-zero rates shown here), however losses to alkenes are significant during both night and day Terpene losses are calculated from GC-MS data, NO & N_2O_5 data are from CRD, and photolysis losses are calculated as described in Section 3.1. Uncertainties in rate constants of BVOC + NO_3 range from 2% for myrcene to - 40% for β-pinene (Calvert et al., 2000). Uncertainties in rate constants of BVOC + NO_3 range from $\pm$ 30% for α-pinene to up to a factor of two for isoprene (Calvert et al., 2000); NO measurements had $\pm$ 35% uncertainty, BVOC measurements $\pm$ 20%, and photolysis $\pm$ 20% based on solar radiation measurement uncertainty.
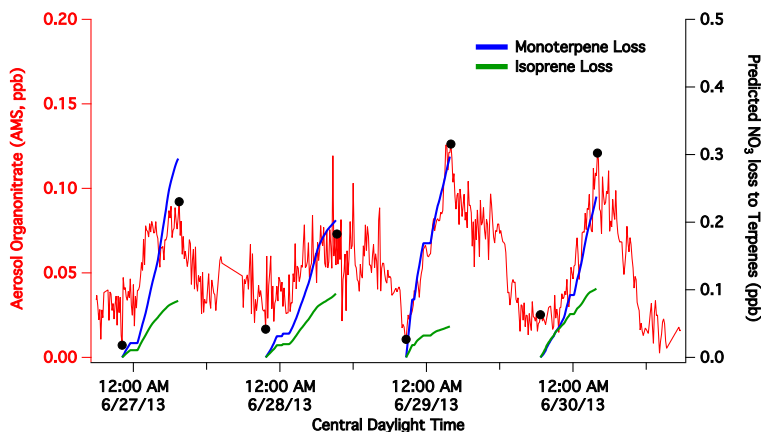

Figure 5. Sample calculation of $(NO_{3,loss})_{integ}$ overlaid against aerosol $RONO_2$ measured by AMS (red). The monoterpene maxima correlate well with the AMS maxima (black dots). Minima and maxima (black dots) were chosen for the beginning and end of AMS buildup periods, respectively. The time period shown is arbitrarily chosen.
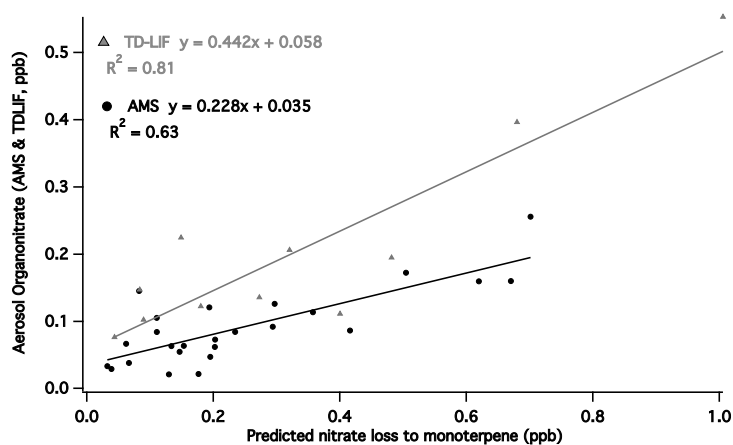
20

Figure 6. Scatter plots of aerosol $RONO_2$ (AMS & TD-LIF) compared to $(NO_{3,loss})_{cum}$. The magnitudes of the two particle phase organic nitrate measurements differ by a factor of $\approx$ 2-4 for unknown reasons, however the slope can be used as a relative molar yield of NO_3 loss to monoterpenes. Time period for AMS comparison is June 9 - July 15, 2013 and for TD-LIF is June 27 - July 15, 2013.
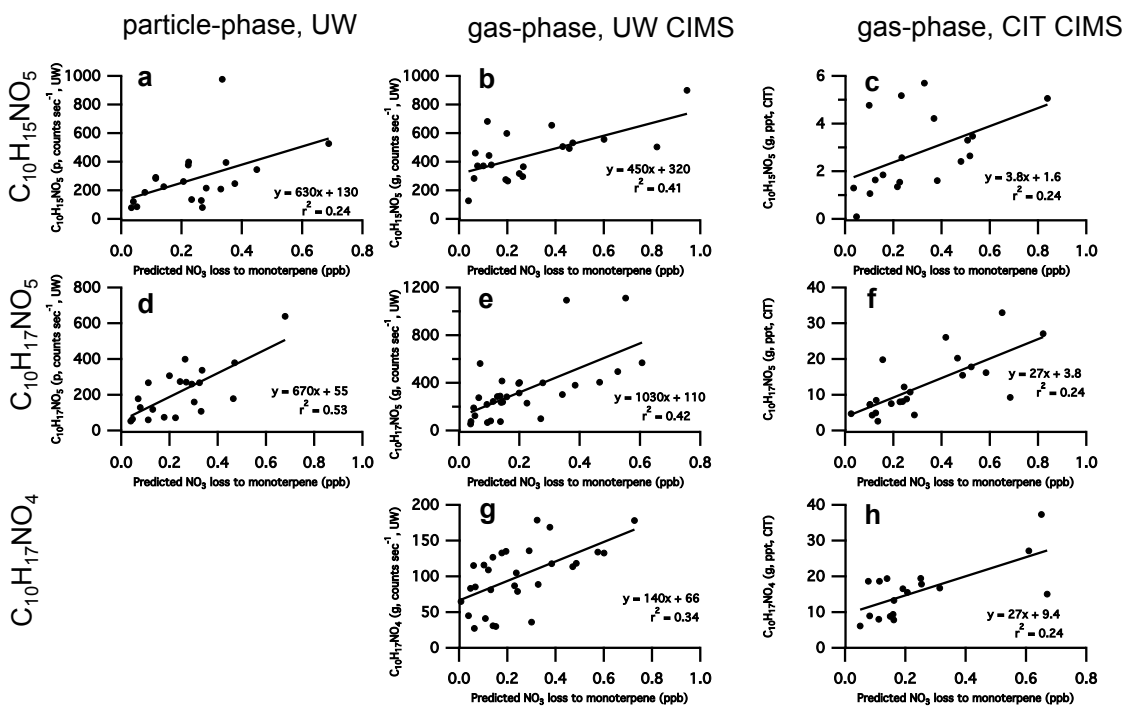
Figure 7. Scatter plots of selected molecules' concentration buildups against time-integrated monoterpene losses to NO_3 radical, during periods of observed organic nitrate buildup measured by CIMS. Panels a & d show particle phase $C_{10}H_{15}NO_5$ and $C_{10}H_{17}NO_5$ measured by the UW FIGAERO; b & e show gas phase $C_{10}H_{15}NO_5$ and $C_{10}H_{17}NO_5$ also measured by UW; c & f show the same gas phase species measured by the CIT-CIMS, with calibrated concentrations. Panels g & h show gas phase $C_{10}H_{17}NO_4$ measured by both CIMS. The gas phase correlations with calibrated mixing ratios measured by the CIT-CIMS (panels c, f, & h) allow for a rough estimation of the lower limit molar yields via the slopes: $C_{10}H_{15}NO_5$, 0.4%; $C_{10}H_{17}NO_5$, 3%; and $C_{10}H_{17}NO_4$, 3%.
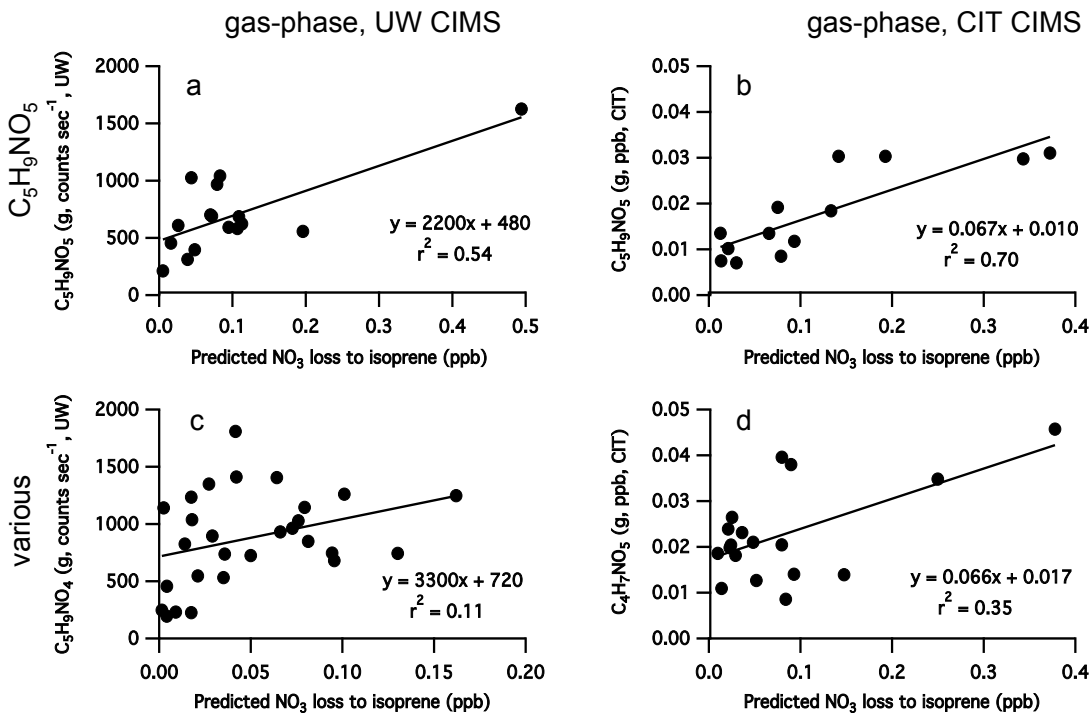
Figure 8. Gas phase CIMS data correlated to predicted isoprene + NO_3, during periods of buildup of these C_5 and C_4 nitrates as measured by each CIMS. Panels a & b show $C_5H_9NO_5$, which is well correlated to predicted isoprene + NO_3 suggesting this is a NO_3 gas phase product, with the calibrated mixing ratios measured by CIT enabling estimation of an approximate lower limit molar yield of 7%. Panel c shows that $C_5H_9NO_4$ is poorly correlated to isoprene + NO_3 suggesting that this product comes (at least in part) from another oxidative source (*e.g.* RO_2+NO). Panel d, $C_4H_7NO_5$, also shows a poorer correlation than panels a & b, suggesting it is not exclusively a product of NO_3 oxidation, or has rapid losses.
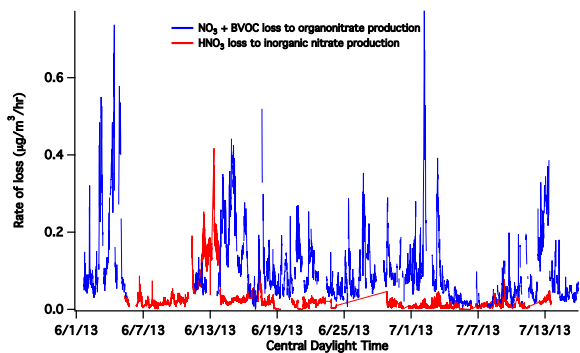

Figure 9. Over the campaign, similar magnitudes of the rate of formation of organic and inorganic nitrate aerosol (according to the pathways shown in Scheme 1) are observed, though peaks occur at different times.

References

Ahmadov, R., McKeen, S. A., Robinson, A. L., Bahreini, R., Middlebrook, A. M., de Gouw, J. A., Meagher, J., Hsie, E.-Y., Edgerton, E., Shaw, S., and Trainer, M.: A volatility basis set model for summertime secondary organic aerosols over the eastern United States in 2006, Journal of Geophysical Research, 117, D06 301, doi:10.1029/2011JD016 831, 2012.

Aldener, M., Brown, S., Stark, H., Williams, E., Lerner, B., Kuster, W., Goldan, P., Quinn, P., Bates, T., and Fehsenfeld, F.: Reactivity and loss mechanisms of NO_3 and N_2O_5 in a polluted marine environment: Results from in situ measurements during New England Air Quality Study 2002, Journal of Geophysical Research: Atmospheres, 111, doi:10.1029/2006JD007 252, 2006.

Allen, H. M., Draper, D. C., Ayres, B. R., Ault, A., Bondy, A., Takahama, S., Modini, R. L., Baumann, K., Edgerton, E., Knote, C., Laskin, A., Wang, B., and Fry, J. L.: Influence of crustal dust and sea spray super-micron particle concentrations and acidity on inorganic NO_3^- aerosol during the 2013 Southern Oxidant and Aerosol Study, Atmospheric Chemistry and Physics, 15, 10 669–10 685, doi:10.5194/acp–15–10 669–2015, 2015.

Atkinson, R. and Arey, J.: Atmospheric Chemistry of Biogenic Organic Compounds, Accounts of Chemical Research, 31, 574–583, 1998.

Atkinson, R. and Arey, J.: Gas-phase tropospheric chemistry of biogenic volatile organic compounds: a review, Atmospheric Environment, 37, 197–219, 2003.

Bahreini, R., Dunlea, E. J., Matthew, B. M., Simons, C., Docherty, K., DeCarlo, P. F., Jimenez, J. L., Brock, C. A., and M.Middlebrook, A.: Design and Operation of a Pressure-Controlled Inlet for Airborne Sampling with an Aerodynamic Aerosol Lens, Aerosol Science and Technology, 42, 465–471, 2008.

Beaver, M. R., Clair, J. M. S., Paulot, F., Spencer, K. M., Crounse, J. D., LaFranchi, B. W., Min, K. E., Pusede, S. E., Wooldridge, P. J., Schade, G. W., Park, C., Cohen, R. C., and Wennberg, P. O.: Importance of biogenic precursors to the budget of organic nitrates: observations of multifunctional organic nitrates by CIMS and TD-LIF during BEARPEX 2009, Atmospheric Chemistry and Physics, 12, 5773–5785, doi:10.5194/acp–12–5773–2012, 2012.

Bellouin, N., Rae, J., Jones, A., Johnson, C., Haywood, J., and Boucher, O.: Aerosol forcing in the Climate Model Intercomparison Project (CMIP5) simulations by HadGEM2-ES and the role of ammonium nitrate, Journal of Geophysical Research, 116, D20 206, doi:10.1029/2011JD016 074, 2011.

Bertram, T. H. and Thornton, J. A.: Toward a general parameterization of N_2O_5 reactivity on aqueous particles: the competing effects of particle liquid water, nitrate and chloride, Atmospheric Chemistry and Physics, 9, 8351–8363, doi:10.5194/acp–9–8351–2009, 2009.

Bertram, T. H., Kimmel, J. R., Crisp, T. A., Ryder, O. S., Yatavelli, R. L. N., Thornton, J. A., Cubison, M. J., Gonin, M., and Worsnop, D. R.: A field-deployable, chemical ionization time-of-flight mass spectrometer, Atmospheric Measurement Techniques, 4, 1471–1479, doi:10.5194/amt–4–1471–2011, 2011.

Blanchard, C., Hidy, G., Tanenbaum, S., and Edgerton, E.: NMOC, ozone, and organic aerosol in the southeastern United States, 1999–2007: 3. Origins of organic aerosol in Atlanta, Georgia, and surrounding areas, Atmospheric Environment, 45, 1291–1302, 2011.

Blanchard, C., Hidy, G., Tanenbaum, S., Edgerton, E., and Hartsell, B.: The Southeastern Aerosol Research and Characterization (SEARCH) study: Temporal trends in gas and PM concentrations and composition, 1999 – 2010, Journal of the Air & Waste Management Association, 63, 247–259, 2013.

Boyd, C., Sanchez, J., Xu, L., Eugene, A., Nah, T., Tuet, W., Guzman, M., , and Ng, N.: Secondary Organic Aerosol (SOA) formation from the β-pinene + NO_3 system: effect of humidity and peroxy radical fate, Atmospheric Chemistry and Physics Discussions, 15, 2679–2744, doi:10.5194/acpd–15–2679–2015, 2015.

Brown, S., Dubé, W., Fuchs, H., Ryerson, T., Wollny, A., Brock, C., Bahreini, R., Middlebrook, A., Neuman, J., and Atlas, E.: Reactive uptake coefficients for N_2O_5 determined from aircraft measurements during the Second Texas Air Quality Study: Comparison to current model parameterizations, Journal of Geophysical Research: Atmospheres, 114, doi:10.1029/2008JD011 679, 2009.

Brown, S., Dubé, W., Peischl, J., Ryerson, T., Atlas, E., Warneke, C., de Gouw, J., te Lintel Hekkert, S., Brock, C., and Flocke, F.: Budgets for nocturnal VOC oxidation by nitrate radicals aloft during the 2006 Texas Air Quality Study, Journal of Geophysical Research: Atmospheres, 116, 2011.

Brown, S. S. and Stutz, J.: Nighttime radical observations and chemistry, Chemical Society Reviews, 41, 6405–6447, 2012.

Brown, S. S., Osthoff, H. D., Stark, H., Dubé, W. P., Ryerson, T. B., Warneke, C., de Gouw, J. A., Wollny, A. G., Parrish, D. D., Fehsenfeld, F. C., and Ravishankara, A. R.: Aircraft observations of daytime NO_3 and N_2O_5 and their implications for tropospheric chemistry, Journal of Photochemistry and Photobiology A: Chemistry, 176, 270–278, 2005.

Brown, S. S., Ryerson, T. B., Wollny, A. G., Brock, C. A., Peltier, R., Sullivan, A. P., Weber, R. J., Dubé, W. P., Trainer, M., Meagher, J. F., Fehsenfeld, F. C., and Ravishankara, A. R.: Variability in nocturnal nitrogen oxide processing and its role in regional air quality, Science, 311, 67–70, 2006.

Calogirou, A., Larsen, B. R., and Kotzias, D.: Gas-phase terpene oxidation products: a review, Atmospheric Environment, 33, 1423–1439, 1999.

Calvert, J. G., Atkinson, R., Kerr, J. A., Madronich, S., Moortgat, G. K., Wallington, T. J., and Yarwood, G.: The Mechanisms of Atmospheric Oxidation of the Alkenes, Oxford University Press, New York, 2000.

Canagaratna, M., Jayne, J., Ghertner, D., Herndon, S., Shi, Q., Jimenez, J., Silva, P., Williams, P., Lanni, T., Drewnick, F., Demerjian, K., Kolb, C., and Worsnop, D.: Chase Studies of Particulate Emissions from in-use New York City Vehicles,, Aerosol Science and Technology, 38, 555–573, 2004.

Carlton, A. G., Pinder, R. W., Bhave, P. V., and Pouliot, G. A.: To What Extent Can Biogenic SOA be Controlled?, Environmental Science & Technology, 44, 3376–3380, 2010.

Chameides, W. L.: Photo-Chemical Role of Tropospheric Nitrogen-Oxides, Geophysical Research Letters, 5, 17–20, 1978.

Cole-Filipiak, N. C., O'Connor, A. E., and Elrod, M. J.: Kinetics of the Hydrolysis of Atmospherically Relevant Isoprene-Derived Hydroxy Epoxides, Environmental Science & Technology, 44, 6718–6723, 2010.

Crounse, J. D., McKinney, K. A., Kwan, A. J., and Wennberg, P. O.: Measurement of Gas-Phase Hydroperoxides by Chemical Ionization Mass Spectrometry, Analytical Chemistry, 78, 6726–6732, 2006.

Crounse, J. D., Nielsen, L. B., and Jørgensen, S.: Autoxidation of Organic Compounds in the Atmosphere, The Journal of Physical Chemistry Letters, 4, 3513–3520, 2013.

Crowley, J. N., Thieser, J., Tang, M. J., Schuster, G., Bozem, H., Beygi, Z. H., Fischer, H., Diesch, J.-M., Drewnick, F., Borrmann, S., Song, W., Yassaa, N., Williams, J., Poehler, D., Platt, U., and Lelieveld, J.: Variable lifetimes and loss mechanisms for NO_3 and N_2O_5 during the DOMINO campaign: contrasts between marine, urban and continental air, Atmospheric Chemistry and Physics, 11, 10 853–10 870, doi:10.5194/acp–11–10 853–2011, 2011.

Crutzen, P. J. and Andreae, M. O.: Biomass Burning in the Tropics - Impact on Atmospheric Chemistry and Biogeochemical Cycles, Science, 250, 1669–1678, 1990.

Dallmann, T., DeMartini, S., Kirchstetter, T., Herndon, S., Onasch, T., Wood, E., and Harley, R.: On-Road measurement of gas and particle phase pollutant emission factors for individual heavy-duty diesel trucks, Environmental Science & Technology, 46, 8511–8518, 2012.

Das, M. and Aneja, V.: Regional analysis of nonmethane volatile organic compounds in the lower troposphere of the Southeast United States, Journal of Environmental Engineering, 129, 1085–1103, 2003.

Day, D. A., Wooldridge, P. J., Dillon, M. B., Thornton, J. A., and Cohen, R. C.: A thermal dissociation laser-induced fluorescence instrument for in situ detection of NO_2, peroxy nitrates, alkyl nitrates, and HNO_3, Journal of Geophysical Research: Atmospheres, 107, 2002.

De Gouw, J. A.: Budget of organic carbon in a polluted atmosphere: Results from the New England Air Quality Study in 2002, Journal of Geophysical Research, 110, D16 305, doi:10.1029/2004JD005 623, 2005.

DeCarlo, P. F., Kimmel, J. R., Trimborn, A., Northway, M. J., Jayne, J. T., Aiken, A. C., Gonin, M., Fuhrer, K., Horvath, T., Docherty, K. S., Worsnop, D. R., and Jimenez, J. L.: Field-deployable, high-resolution, time-of-flight aerosol mass spectrometer, Analytical Chemistry, 78, 8281–8289, 2006.

Dentener, F. J. and Crutzen, P. J.: Reaction of N_2O_5 on tropospheric aerosols: Impact on the global distributions of NO_x, O_3, and OH, Journal of Geophysical Research: Atmospheres, 98, 7149–7163, 1993.

Draper, D. C., Farmer, D. K., and Fry, J. L.: A comparison of Secondary Organic Aerosol (SOA) yields and composition from ozonolysis of monoterpenes at varying concentrations of NO_2, Atmospheric Chemistry and Physics Discussions, 15, 14 923–14 960, doi:10.5194/acpd–15–14 923–2015, 2015.

Dubé, W. P., Brown, S. S., Osthoff, H. D., Nunley, M. R., Ciciora, S. J., Paris, M. W., McLaughlin, R. J., and Ravishankara, A. R.: Aircraft instrument for simultaneous, in situ measurement of NO_3 and N_2O_5 via pulsed cavity ring-down spectroscopy, Review Of Scientific Instruments, 77, 034 101, 2006.

Eddingsaas, N., Loza, C., Yee, L., Seinfeld, J., and Wennberg, P.: α-pinene photooxidation under controlled chemical conditions–Part 1: Gas-phase composition in low- and high-NO_x environments, Atmospheric Chemistry and Physics, 12, 6489–6504, doi:10.5194/acp–10 12–6489–2012, 2012.

Epstein, S. A., Blair, S. L., and Nizkorodov, S. A.: Direct Photolysis of α-Pinene Ozonolysis Secondary Organic Aerosol: Effect on Particle Mass and Peroxide Content, Environmental Science & Technology, 48, 11 251–11 258, 2014.

Evans, M. J. and Jacob, D. J.: Impact of new laboratory studies of N_2O_5 hydrolysis on global model budgets of tropospheric nitrogen oxides, ozone, and OH, Geophysical Research Letters, 32, L09 813, 2005.

Farmer, D., Matsunaga, A., Docherty, K., Surratt, J., Seinfeld, J., Ziemann, P., and Jimenez, J.: Response of an aerosol mass spectrometer to organonitrates and organosulfates and implications for atmospheric chemistry, Proceedings of the National Academy of Sciences, 107, 6670–6675, 2010.

Feng, Y. and Penner, J. E.: Global modeling of nitrate and ammonium: Interaction of aerosols and tropospheric chemistry, Journal of Geophysical Research: Atmospheres, 112, D01 304, doi:10.1029/2005JD006 404, 2007.

Fry, J. L., Kiendler-Scharr, A., Rollins, A. W., Wooldridge, P. J., Brown, S. S., Fuchs, H., Dubé, W., Mensah, A., Dal Maso, M., Tillmann, R., Dorn, H.-P., Brauers, T., and Cohen, R. C.: Organic nitrate and secondary organic aerosol yield from NO_3 oxidation of β-pinene evaluated using a gas-phase kinetics/aerosol partitioning model, Atmospheric Chemistry and Physics, 9, 1431, doi:10.5194/acp–9–1431–2009, 2009.

Fry, J. L., Kiendler-Scharr, A., Rollins, A. W., Brauers, T., Brown, S. S., Dorn, H.-P., Dubé, W. P., Fuchs, H., Mensah, A., Rohrer, F., Tillmann, R., Wahner, A., Wooldridge, P. J., and Cohen, R. C.: SOA from limonene: role of NO_3 in its generation and degradation, Atmospheric Chemistry and Physics, 11, 3879, doi:10.5194/acp–11–3879–2011, 2011.

Fry, J. L., Draper, D. C., Zarzana, K. J., Campuzano-Jost, P., Day, D. A., Jimenez, J. L., Brown, S. S., Cohen, R. C., Kaser, L., and Hansel, A.: Observations of gas-and aerosol-phase organic nitrates at BEACHON-RoMBAS 2011, Atmospheric Chemistry and Physics, 13, 1979–2034, doi:10.5194/acpd–13–1979–2013, 2013.

Fry, J. L., Draper, D. C., Barsanti, K. C., Smith, J. N., Ortega, J., Winkler, P. M., Lawler, M. J., Brown, S. S., Edwards, P. M., Cohen, R. C., and Lee, L.: Secondary Organic Aerosol Formation and Organic Nitrate Yield from NO_3 Oxidation of Biogenic Hydrocarbons, Environmental Science & Technology, 48, 11 944–11 953, 2014.

Galloway, J., Dentener, F., Capone, D., Boyer, E., Howarth, R., Seitzinger, S., Asner, G., Cleveland, C., Green, P., and Holland, E.: Nitrogen cycles: past, present, and future, Biogeochemistry, 70, 153–226, 2004.

Geron, C., Rasmussen, R., Arnts, R. R., and Guenther, A.: A review and synthesis of monoterpene speciation from forests in the United States, Atmospheric Environment, 34, 1761–1781, 2000.

Geyer, A., Alicke, B., Konrad, S., Schmitz, T., Stutz, J., and Platt, U.: Chemistry and oxidation capacity of the nitrate radical in the continental boundary layer near Berlin, Journal of Geophysical Research: Atmospheres, 106, 8013–8025, 2001.

Gilman, J. B., Burkhart, J. F., Lerner, B. M., Williams, E. J., Kuster, W. C., Goldan, P. D., Murphy, P. C., Warneke, C., Fowler, C., Montzka, S. A., Miller, B. R., Miller, L., Oltmans, S. J., Ryerson, T. B., Cooper, O. R., Stohl, A., and de Gouw, J. A.: Ozone variability and halogen oxidation within the Arctic and sub-Arctic springtime boundary layer, Atmospheric Chemistry and Physics, 10, 10 223–10 236, doi:10.5194/acp–10–10 223–2010, 2010.

Goldan, P. D., Kuster, W. C., Fehsenfeld, F. C., and Montzka, S. A.: Hydrocarbon measurements in the southeastern United States: The Rural Oxidants in the Southern Environment (ROSE) Program 1990, Journal of Geophysical Research: Atmospheres, 100, 25 945, 10.1029/95JD02 607, 1995.

Goldan, P. D., Kuster, W. C., Williams, E., Murphy, P. C., Fehsenfeld, F. C., and Meagher, J.: Nonmethane hydrocarbon and oxy hydrocarbon measurements during the 2002 New England Air Quality Study, Journal of Geophysical Research: Atmospheres, 109, doi:10.1029/2003JD004 455, 2004.

Goldstein, A., Koven, C., Heald, C., and Fung, I.: Biogenic carbon and anthropogenic pollutants combine to form a cooling haze over the southeastern United States, Proceedings of the National Academy of Sciences, 106, 8835–8840, 2009.

Goldstein, A. H. and Galbally, I. E.: Known and unexplored organic constituents in the earth's atmosphere, Environmental Science & Technology, 41, 1514–1521, 2007.

Griffin, R. J., Cocker, D. R., III, Flagan, R. C., and Seinfeld, J. H.: Organic aerosol formation from the oxidation of biogenic hydrocarbons, Journal of Geophysical Research: Atmospheres, 104, 3555–3567, 1999.

620 Hallquist, M., Wängberg, I., Ljungström, E., Barnes, I., and Becker, K.: 121 2009 Aerosol and product yields from NO_3 radical-initiated oxidation of selected monoterpenes, Environmental Science & Technology, 33, 553–559, 1999.

Hallquist, M., Wenger, J. C., Baltensperger, U., Rudich, Y., Simpson, D., Claeys, M., Dommen, J., Donahue, N. M., George, C., Goldstein, A. H., Hamilton, J. F., Herrmann, H., Hoffmann, T., Iinuma, Y., Jang, M.,

625 Jenkin, M. E., Jimenez, J. L., Kiendler-Scharr, A., Maenhaut, W., McFiggans, G., Mentel, T. F., Monod, A., Prévôt, A. S. H., Seinfeld, J. H., Surratt, J. D., Szmigielski, R., and Wildt, J.: The formation, properties and impact of secondary organic aerosol: current and emerging issues, Atmospheric Chemistry and Physics, 9, 5155–5236, doi:10.5194/acp–9–5155–2009, 2009.

Heald, C. L., Jacob, D. J., Park, R. J., Russell, L. M., Huebert, B. J., Seinfeld, J. H., Liao, H., and Weber, R. J.:

630 A large organic aerosol source in the free troposphere missing from current models, Geophysical Research Letters, 32, L18 809, doi:10.1029/2005GL023 831, 2005.

Hidy, G. M., Blanchard, C. L., Baumann, K., Edgerton, E., Tanenbaum, S., Shaw, S., Knipping, E., Tombach, I., Jansen, J., and Walters, J.: Chemical climatology of the southeastern United States, 1999–2013, Atmospheric Chemistry and Physics, 14, 11 893–11 914, doi:10.5194/acp–14–11 893–2014, 2014.

635 Horowitz, L. W., Fiore, A. M., Milly, G. P., Cohen, R. C., Perring, A., Wooldridge, P. J., Hess, P. G., Emmons, L. K., and Lamarque, J.-F.: Observational constraints on the chemistry of isoprene nitrates over the eastern United States, Journal of Geophysical Research: Atmospheres, 112, 2007.

Hu, W. W., Campuzano-Jost, P., Palm, B. B., Day, D. A., Ortega, A. M., Hayes, P. L., Krechmer, J. E., Chen, Q., Kuwata, M., Liu, Y. J., de Sá, S. S., Martin, S. T., Hu, M., Budisulistiorini, S. H., Riva, M., Surratt, J. D.,

640 St. Clair, J. M., Isaacman-Van Wertz, G., Yee, L. D., Goldstein, A. H., Carbone, S., Artaxo, P., de Gouw, J. A., Koss, A., Wisthaler, A., Mikoviny, T., Karl, T., Kaser, L., Jud, W., Hansel, A., Docherty, K. S., Robinson, N. H., Coe, H., Allan, J. D., Canagaratna, M. R., Paulot, F., and Jimenez, J. L.: Characterization of a real-time tracer for Isoprene Epoxydiols-derived Secondary Organic Aerosol (IEPOX-SOA) from aerosol mass spectrometer measurements, Atmospheric Chemistry and Physics, in press, 2015.

645 Jimenez, J. L., Canagaratna, M. R., Donahue, N. M., Prevot, A. S. H., Zhang, Q., Kroll, J. H., DeCarlo, P. F., Allan, J. D., Coe, H., Ng, N. L., Aiken, A. C., Docherty, K. S., Ulbrich, I. M., Grieshop, A. P., Robinson, A. L., Duplissy, J., Smith, J. D., Wilson, K. R., Lanz, V. A., , Hueglin, C., Sun, Y. L., , Tian, J., Laaksonen, A., Raatikainen, T., Rautiainen, J., Vaattovaara, P., Ehn, M., Kulmala, M., , Tomlinson, J. M., Collins, D. R., Cubison, M. J., Dunlea, E. J., Huffman, J. A., Onasch, T. B., Alfarra, M. R., , , Williams, P. I., , Bower, K.,

650 Kondo, Y., Schneider, J., Drewnick, F., , Borrmann, S., , Weimer, S., , , Demerjian, K., Salcedo, D., Cottrell, L., Griffin, R., , Takami, A., Miyoshi, T., Hatakeyama, S., Shimono, A., Sun, J. Y., Zhang, Y. M., Dzepina, K., , Kimmel, J. R., , , , Sueper, D., , Jayne, J. T., Herndon, S. C., Trimborn, A. M., Williams, L. R., Wood, E. C., Middlebrook, A. M., Kolb, C. E., Baltensperger, U., and Worsnop, D. R.: Evolution of organic aerosols in the atmosphere, Science, 326, 1525–1529, 2009.

28

655 Kroll, J. H. and Seinfeld, J. H.: Chemistry of secondary organic aerosol: Formation and evolution of low-volatility organics in the atmosphere, Atmospheric Environment, 42, 3593–3624, 2008.

Lee, A. K. Y., Herckes, P., Leaitch, W. R., Macdonald, A. M., and Abbatt, J. P. D.: Aqueous OH oxidation of ambient organic aerosol and cloud water organics: Formation of highly oxidized products, Geophysical Research Letters, 38, L11 805, 2011.

660 Lee, B. H., Lopez-Hilfiker, F. D., Mohr, C., Kurtén, T., Worsnop, D. R., and Thornton, J. A.: An Iodide-Adduct High-Resolution Time-of-Flight Chemical-Ionization Mass Spectrometer: Application to Atmospheric Inorganic and Organic Compounds, Environmental Science & Technology, 48, 6309–6317, 2014.

Lee, B. H., Mohr, C., Lopez-Hilfiker, F. D., Lutz, A., Hallquist, M., Hu, W. W., Jimenez, J., Xu, L., Ng, N. L., Romer, P., Cohen, R. C., Wild, R. J., Kim, S., de Gouw, J., Goldstein, A. H., Shepson, P. B., Wennberg,
665 P. O., and Thornton, J. A.: Highly functionalized particle-phase organic nitrates observed in the Southeastern U.S.: contribution to secondary organic aerosol and reactive nitrogen budgets, submitted to Proceedings of the National Academy of Sciences, 2015.

Lee, T., Yu, X.-Y., Ayres, B., Kreidenweis, S., Malm, W., and Collett Jr, J.: Observations of fine and coarse particle nitrate at several rural locations in the United States, Atmospheric Environment, 42, 2720–2732,
670 2008.

Liu, S., Shilling, J. E., Song, C., Hiranuma, N., Zaveri, R. A., and Russell, L. M.: Hydrolysis of Organonitrate Functional Groups in Aerosol Particles, Aerosol Science and Technology, 46, 1359–1369, 2012.

Lopez-Hilfiker, F. D., Mohr, C., Ehn, M., Rubach, F., Kleist, E., Wildt, J., Mentel, T. F., Lutz, A., Hallquist, M., Worsnop, D., and Thornton, J. A.: A novel method for online analysis of gas and particle composition:
675 description and evaluation of a Filter Inlet for Gases and AEROsols (FIGAERO), Atmospheric Measurement Techniques, 7, 983–1001, doi:10.5194/amt–7–983–2014, 2014.

Makkonen, U., Virkkula, A., Mantykentta, J., Hakola, H., Keronen, P., Vakkari, V., and Aalto, P. P.: Semi-continuous gas and inorganic aerosol measurements at a Finnish urban site: comparisons with filters, nitrogen in aerosol and gas phases, and aerosol acidity, Atmospheric Chemistry and Physics, 12, 5617–5631,
680 doi:10.5194/acp–12–5617–2012, 2012.

Müller, J.-F., Peeters, J., and Stavrakou, T.: Fast photolysis of carbonyl nitrates from isoprene, Atmospheric Chemistry and Physics, 14, 2497–2508, 2014.

Myhre, G., Samset, B. H., Schulz, M., Balkanski, Y., Bauer, S., Berntsen, T. K., Bian, H., Bellouin, N., Chin, M., Diehl, T., Easter, R. C., Feichter, J., Ghan, S. J., Hauglustaine, D., Iversen, T., Kinne, S., Kirkevåg, A.,
685 Lamarque, J. F., Lin, G., Liu, X., Lund, M. T., Luo, G., Ma, X., van Noije, T., Penner, J. E., Rasch, P. J., Ruiz, A., Seland, Ø., Skeie, R. B., Stier, P., Takemura, T., Tsigaridis, K., Wang, P., Wang, Z., Xu, L., Yu, H., Yu, F., Yoon, J. H., Zhang, K., Zhang, H., and Zhou, C.: Radiative forcing of the direct aerosol effect from AeroCom Phase II simulations, Atmospheric Chemistry and Physics, 13, 1853–1877, doi:10.5194/acp–13–1853–2013, 2013.

690 Nel, A.: Atmosphere. Air pollution-related illness: effects of particles., Science, 308, 804–806, 2005.

Nguyen, T. B., Crounse, J. D., Teng, A. P., Clair, J. M. S., Paulot, F., Wolfe, G. M., and Wennberg, P. O.: Rapid deposition of oxidized biogenic compounds to a temperate forest, Proceedings of the National Academy of Sciences, 112, E392–E401, 2015.

29

Nizich, S. V., Pope, A. A., Driver, L. M., and Pechan-Avanti Group: NATIONAL AIR POLLUTANT EMIS-
SION TRENDS,1900 - 1998, Tech. rep., Environmental Protection Agency, 2000.

Odman, M. T., Boylan, J. W., and Russell, A. G.: Air Pollution Modeling and Its Application XVI, Springer
Science+Business Media New York, 16 edn., 2004.

Perring, A. E., Pusede, S. E., and Cohen, R. C.: An Observational Perspective on the Atmospheric Impacts
of Alkyl and Multifunctional Nitrates on Ozone and Secondary Organic Aerosol, Chemical Reviews, 113,
5848–5870, 2013.

Pope, C. A. and Dockery, D. W.: Health effects of fine particulate air pollution: Lines that connect, Journal of
the Air & Waste Management Association, 56, 709–742, 2006.

Pye, H. O. T., Chan, A. W. H., Barkley, M. P., and Seinfeld, J. H.: Global modeling of organic aerosol: the
importance of reactive nitrogen (NO_x and NO_3), Atmospheric Chemistry and Physics, 10, 11 261–11 276,
doi:10.5194/acp–10–11 261–2010, 2010.

Riemer, N., Vogel, H., Vogel, B., Anttila, T., Kiendler-Scharr, A., and Mentel, T. F.: Relative importance of
organic coatings for the heterogeneous hydrolysis of N_2O_5 during summer in Europe, Journal of Geophysical
Research: Atmospheres, 114, D17 307, 2009.

Rollins, A. W., Smith, J. D., Wilson, K. R., and Cohen, R. C.: Real time in situ detection of organic nitrates in
atmospheric aerosols, Environmental Science & Technology, 44, 5540–5545, 2010.

Rollins, A. W., Browne, E. C., Min, K.-E., Pusede, S. E., Wooldridge, P. J., Gentner, D. R., Goldstein, A. H., Liu,
S., Day, D. A., Russell, L. M., and Cohen, R. C.: Evidence for NOx Control over Nighttime SOA Formation,
Science, 337, 1210, doi:10.1126/science.1221 520, 2012.

Sander, S. P., Friedl, R. R., Barker, J. R., Golden, D. M., Kurylo, M. J., Wine, P. H., Abbatt, J. P. D., Burkholder,
J. B., Kolb, C. E., Moortgat, G. K., Huie, R. E., and Orkin, V. L.: Chemical Kinetics and Photochemical Data
for Use in Atmospheric Studies - Evaluation Number 17, JPL Publication 10-6, Pasadena, California, pp.
1–684, 2011.

Saunders, S. M., Jenkin, M. E., Derwent, R. G., and Pilling, M. J.: Protocol for the development of the Master
Chemical Mechanism, MCM v3 (Part A): tropospheric degradation of non-aromatic volatile organic com-
pounds, Atmospheric Chemistry and Physics, 3, 161–180, doi:10.5194/acp–3–161–2003, 2003.

Seinfeld, J. H. and Pandis, S. N.: Atmospheric Chemistry and Physics: From Air Pollution to Climate Change,
John Wiley Sons, Inc. Hoboken, New Jersey, second edn., 2006.

Spittler, M., Barnes, I., Bejan, I., Brockmann, K., Benter, T., and Wirtz, K.: Reactions of NO_3 radicals with
limonene and α-pinene: Product and SOA formation, Atmospheric Environment, 40, S116–S127, 2006.

Spracklen, D. V., Jimenez, J. L., Carslaw, K. S., Worsnop, D. R., Evans, M. J., Mann, G. W., Zhang, Q.,
Canagaratna, M. R., Allan, J., Coe, H., McFiggans, G., Rap, A., and Forster, P.: Aerosol mass spectrometer
constraint on the global secondary organic aerosol budget, Atmospheric Chemistry and Physics, 11, 12 109–
12 136, doi:10.5194/acp–11–12 109–2011, 2011.

Stanier, C. O., Khlystov, A. Y., Chan, W. R., Mandiro, M., and Pandis, S. N.: A method for the in situ measure-
ment of fine aerosol water content of ambient aerosols: The dry-ambient aerosol size spectrometer (DAASS),
Aerosol Science and Technology, 38, 215–228, 2004.

Stocker, T. F., Qin, D., Plattner, G.-K., Tignor, M. M. B., Allen, S. K., Boschung, J., Nauels, A., Xia, Y., Bex, V.,
and Midgley, P. M., eds.: Climate Change 2013: The Physical Science Basis, Working Group I Contribution

to the Fifth Assessment Report of the Intergovernmental Panel on Climate Change, Cambridge University Press, Cambridge, UK, 2013.

Stroud, C., Roberts, J., Williams, E., Hereid, D., Angevine, W., Fehsenfeld, F., Wisthaler, A., Hansel, A., Martinez-Harder, M., Harder, H., Brune, W., Hoenninger, G., Stutz, J., and White, A.: Nighttime isoprene trends at an urban forested site during the 1999 Southern Oxidant Study, Journal of Geophysical Research-Atmospheres, 107, D16, doi:10.1029/2001JD000 959, 2002.

Trebs, I., Meixner, F. X., Slanina, J., Otjes, R., Jongejan, P., and Andreae, M. O.: Real-time measurements of ammonia, acidic trace gases and water-soluble inorganic aerosol species at a rural site in the Amazon Basin, Atmospheric Chemistry and Physics, 4, 967–987, doi:10.5194/acp–4–967–2004, 2004.

Vlasenko, A., Sjogren, S., Weingartner, E., Stemmler, K., Gaggeler, H. W., and Ammann, M.: Effect of humidity on nitric acid uptake to mineral dust aerosol particles, Atmospheric Chemistry and Physics, 6, 2147–2160, doi:10.5194/acp–6–2147–2006, 2006.

von Kuhlmann, R., Lawrence, M. G., Pöschl, U., and Crutzen, P. J.: Sensitivities in global scale modeling of isoprene, Atmospheric Chemistry and Physics, 4, 1–17, 2004.

Wagner, N. L., Dubé, W. P., Washenfelder, R. A., Young, C. J., Pollack, I. B., Ryerson, T. B., , and Brown, S. S.: Diode laser-based cavity ring-down instrument for NO_3, N_2O_5, NO, NO_2 and O_3 from aircraft, Atmospheric Measurement Techniques, 4, 1227–1240, doi:10.5194/amt–4–1227–2011, 2011.

Wagner, N. L., Riedel, T. P., Young, C. J., Bahreini, R., Brock, C. A., Dubé, W. P., Kim, S., Middlebrook, A. M., Öztürk, F., Roberts, J. M., Russo, R., Sive, B., Swarthout, R., Thornton, J. A., VandenBoer, T. C., Zhou, Y., and Brown, S. S.: N_2O_5 uptake coefficients and nocturnal NO_2 removal rates determined from ambient wintertime measurements, Journal of Geophysical Research: Atmospheres, 118, 9331–9350, 2013.

Warneke, C., De Gouw, J. A., Goldan, P. D., Kuster, W. C., Williams, E. J., Lerner, B. M., Jakoubek, R., Brown, S. S., Stark, H., Aldener, M., Ravishankara, A. R., Roberts, J. M., Marchewka, M., Bertman, S., Sueper, D. T., McKeen, S. A., Meagher, J. F., and Fehsenfeld, F. C.: Comparison of daytime and nighttime oxidation of biogenic and anthropogenic VOCs along the New England coast in summer during New England Air Quality Study 2002, Journal of Geophysical Research: Atmospheres, 109, 2004.

Wayne, R., Barnes, I., Biggs, P., Burrows, J., Canosa-Mas, C., Hjorth, J., Le Bras, G., Moortgat, G., Perner, D., and Poulet, G.: The nitrate radical: Physics, chemistry, and the atmosphere, Atmospheric Environment. Part A. General Topics, 25, 1–203, 1991.

Wild, R., Edwards, P., Dubé, W., Baumann, K., Edgerton, E., Quinn, P., Roberts, J., Rollins, A., Veres, P., Warneke, C., Williams, E., Yuan, B., and Brown, S.: A Measurement of Total Reactive Nitrogen, NO_y, together with NO_2, NO and O_3 via Cavity Ring-Down Spectroscopy, Environmental Science & Technology, 48, 9609–9615, 2014.

Winer, A. M., Atkinson, R., and James N. Pitts, J.: Gaseous Nitrate Radical: Possible Nighttime Atmospheric Sink for Biogenic Organic Compounds, Science, 224, 156–159, 1984.

Xie, Y., Paulot, F., Carter, W. P. L., Nolte, C. G., Luecken, D. J., Hutzell, W. T., Wennberg, P. O., Cohen, R. C., and Pinder, R. W.: Understanding the impact of recent advances in isoprene photooxidation on simulations of regional air quality, Atmospheric Chemistry and Physics, 13, 8439–8455, 2013.

Xu, L., Guo, H., Boyd, C. M., Klein, M., Bougiatioti, A., Cerully, K. M., Hite, J. R., Isaacman-VanWertz, G., Kreisberg, N. M., Knote, C., Olson, K., Koss, A., Goldstein, A. H., Hering, S. V., de Gouw, J., Baumann, K.,

Lee, S.-H., Nenes, A., Weber, R. J., and Ng, N. L.: Effects of anthropogenic emissions on aerosol formation
775   from isoprene and monoterpenes in the southeastern United States, Proceedings of the National Academy of
Sciences, 112, 37–42, 2015a.

Xu, L., Suresh, S., Guo, H., Weber, R. J., and Ng, N. L.: Aerosol characterization over the southeastern United
States using high-resolution aerosol mass spectrometry: spatial and seasonal variation of aerosol composition
and sources with a focus on organic nitrates, Atmospheric Chemistry and Physics, 15, 7307–7336, 2015b.

780 Yatavelli, R., Lopez-Hilfiker, F., Wargo, J., Kimmel, J., Cubison, M., Bertram, T., Jimenez, J., Gonin, M.,
Worsnop, D., and Thornton, J.: A Chemical Ionization High-Resolution Time-of-Flight Mass Spectrometer
Coupled to a Micro Orifice Volatilization Impactor (MOVI-HRToF-CIMS) for Analysis of Gas and Particle-
Phase Organic Species, Aerosol Science and Technology, 46, 1313–1327, 2012.

Zhang, Q., Jimenez, J. L., Canagaratna, M. R., Allan, J. D., Coe, H., Ulbrich, I., Alfarra, M. R., Takami,
785   A., Middlebrook, A. M., Sun, Y. L., Dzepina, K., Dunlea, E., Docherty, K., DeCarlo, P. F., Salcedo, D.,
Onasch, T., Jayne, J. T., Miyoshi, T., Shimono, A., Hatakeyama, S., Takegawa, N., Kondo, Y., Schneider,
J., Drewnick, F., Borrmann, S., Weimer, S., Demerjian, K., Williams, P., Bower, K., Bahreini, R., Cottrell,
L., Griffin, R. J., Rautiainen, J., Sun, J. Y., Zhang, Y. M., and Worsnop, D. R.: Ubiquity and dominance of
oxygenated species in organic aerosols in anthropogenically-influenced Northern Hemisphere midlatitudes,
790   Geophysical Research Letters, 34, L13 801. doi:10.1029/2007GL029 979, 2007.